

Linear Local Stability of Electrostatic Drift Modes in Helical Systems

YAMAGISHI Osamu, NAKAJIMA Noriyoshi, SUGAMA Hideo and NAKAMURA Yuji¹

National Institute for Fusion Science, Toki, 509-5292, Japan

¹*Graduate School of Energy Science, Kyoto University, Uji, 611-0011, Japan*

(Received: 9 December 2003 / Accepted: 20 April 2004)

Abstract

Linear local gyrokinetic-Poisson equations are solved numerically, to investigate the stability of collisionless electrostatic drift modes in a helical system. As a model of helical plasmas, Large Helical Device (LHD) is considered, whose MHD equilibrium is numerically obtained. A circular tokamak with comparable aspect ratio to that of the LHD is also considered for comparison. As electrostatic drift wave branches, ion temperature gradient modes (ITG), trapped electron modes (TEM), and electron temperature gradient modes (ETG) can become unstable. For these modes, the local parameter dependence is investigated and destabilizing mechanisms are discussed in an LHD configuration.

Keywords:

linear gyrokinetics, ITG, TEM, ETG, helical system

1. Introduction

Drift wave instabilities are considered to cause a large amount of the transport and it is important to investigate their stability properties. Many investigations have been done for tokamaks, while there seem to be only numerable studies for helical plasmas. There exist many helical devices with a wide variety of geometry and magnetic field structure, so that it is important to investigate the stability in each helical systems and integrate the results, in order to discuss what is common and what is inherent feature in many configurations including tokmaks. Thus we investigate the stability of the drift wave in a helical system, Large Helical Device (LHD) [1], and try to obtain the driving mechanisms of each linear instability. For this purpose, we solve the linear local gyrokinetic-Poisson equations in the electrostatic regime. The equation we apply is rather exact in the framework of linear gyrokinetic theory [2,3], where the ballooning representation is used as a minimal approximation. Here we consider only collisionless cases. In this formulation, the non-adiabatic dynamics of circulating and trapped electrons/ions is formally treated without any assumptions in all the frequency regime. Then, as different drift branches, ion temperature gradient modes (ITG), trapped electron modes (TEM), and electron temperature gradient modes (ETG) can be considered without missing the correlation between them.

The model MHD equilibria are numerically calculated by VMEC code with a fixed boundary constraint [4]. The net current is assumed to be zero for LHD. The temperature and density profile are prescribed as a function of normalized

toroidal flux, s , as $T/T(0) = 1 - s$ and $n/n(0) = (1 - s)^{0.2}$, where $n_i = n_e$ and $T_i = T_e$ are assumed below. Then $p = 2nT$ is used as an input for VMEC code. The central beta ($\beta_0 \equiv 2\mu_0 p(0)/B_0^2$) is 1.0 %, where β_0 is averaged magnetic field strength at $R = R_0 = 3.75$ [m]. The measure of temperature gradient, $\eta = d \ln T / d \ln n = 1/a = 5$ holds everywhere, and sufficient instabilities are expected for this value. For comparison, we also consider a circular tokamak with comparable aspect ratio $R_0/a = 3.9/0.57$ to the LHD, for which q profile is assumed to be the same as that in the currentless LHD.

2. ITG cases

In Fig. 1, the $k_{\perp} \rho_{thi}$ dependence of the frequencies is shown for LHD, to investigate the ion finite Larmor radius (FLR) effect. Here $\rho_{thi} \equiv v_{thi}/\Omega_i$ and $k_{\perp} = n_k |k/k_{\alpha}|$ with n_k being a toroidal mode number, and $|k/k_{\alpha}|$ is treated as an equilibrium quantity with a fixed ballooning angle θ_k [2]. A case for non-adiabatic electrons and ions is shown by closed circles. The mode can also be destabilized by only non-adiabatic ions which is shown by open circles. This and negative real frequency indicate that the modes are the ITG. From the comparison of the cases with or without the non-adiabatic electrons, it can be seen that the non-adiabatic electrons are destabilization for the ITG, and this can be explained such that the fraction of stabilizing adiabatic electrons is reduced. We also plot a case that the magnetic drift frequency ω_d is ignored in the gyrokinetic equation,

which is denoted by triangles in Fig. 1. Since the curvature of a field line is entered only through ω_d , the residual instabilities are driven by slab-like, parallel compressibility. The growth rate is reduced by ignoring the ω_d , but the instabilities still remain unstable.

In Fig. 2(a), the radial dependence of the ITG frequencies is shown as a function of normalized toroidal flux s , for LHD and a tokamak with a comparable aspect ratio. Here we consider a fixed toroidal mode number n_k , and it is chosen as $n_k = 86$ for LHD and $n_k = 142$ for tokamak, such that $k_{\perp}\rho_{thi}(\theta = 0)$ value is comparable at a fixed radial label. The value of $k_{\perp}\rho_{thi}$ is also shown on right Y-axis in Fig. 2(a), which is large at the core and small at the edge depending mainly on the temperature. For LHD and the tokamak, it can be seen that the frequency dependence is not so different. We also plot the α dependence of the frequencies in Fig. 2(b), where change of α affects the local curvature and local shear

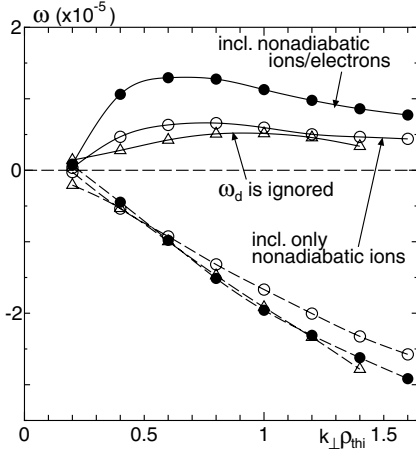


Fig. 1 $k_{\perp}\rho_{thi}$ dependence of ITG frequencies in LHD. Real frequency and growth rate are shown by dashed and solid line respectively. Local parameters are $(s, \theta_k, M\alpha) = (0.7, 0, \pi)$. Closed circles are for a case of non-adiabatic ions and electrons, and open circles are for a case of eliminating non-adiabatic electrons. Triangles are for a case of ignoring ω_d .

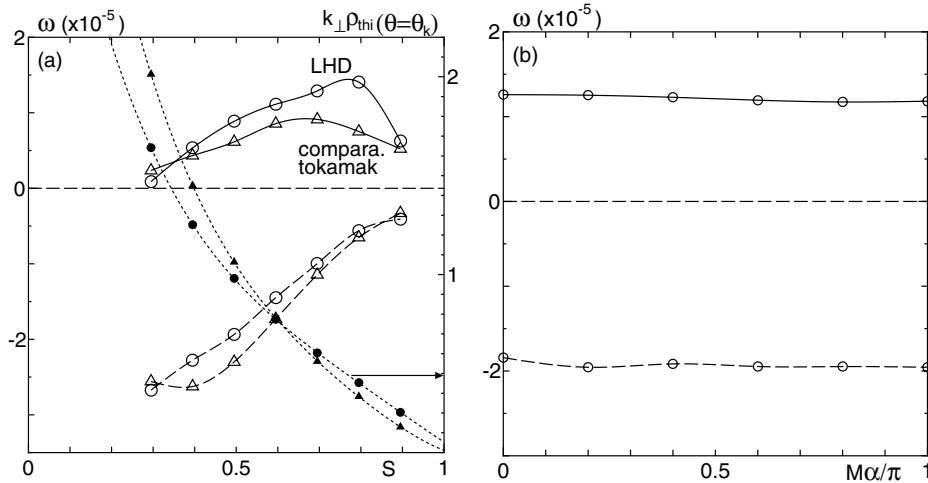


Fig. 2 (a) Radial dependence of ITG frequencies in LHD (circles) and tokamak (triangles) with $\theta_k = 0$ and $M\alpha = \pi$. (b) Field line dependence of ITG frequency in LHD with $s = 0.7$ and $\theta_k = 0$. Real frequency and growth rate are shown by dashed and solid line respectively. In (a), $k_{\perp}\rho_{thi}(\theta = 0)$ value is also plotted by dotted line for right coordinate.

in the toroidal direction in non-axisymmetric systems through the change of field line label. Here M in the figure denotes a number of field periods ($M = 10$ for LHD). The equilibrium and linear instabilities are $2\pi/M$ periodic in α and it is negligible in the axisymmetric case. It can be seen that the α dependence is found to be very weak in LHD.

The value of flux surface quantities like q , q' is changed

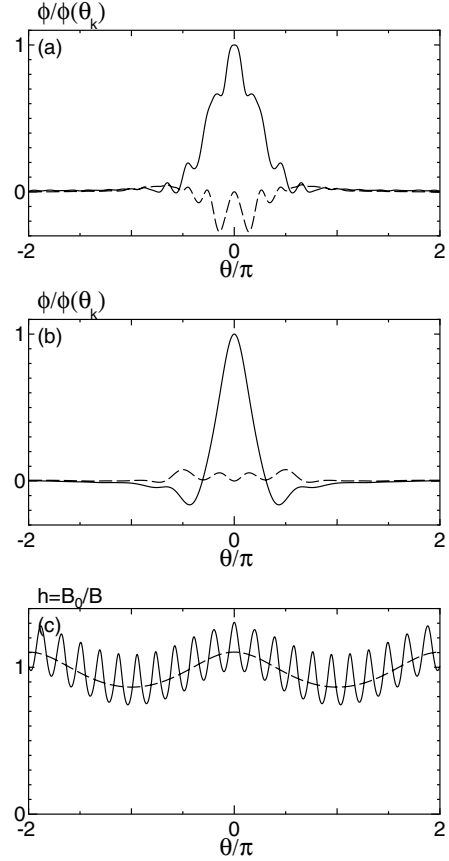


Fig. 3 ITG eigenfunction ϕ for (a) LHD and (b) comparable ε_t tokamak, at $s = 0.7$ and $k_{\perp}\rho_{thi}(\theta = 0) = 0.6$. Real (imaginary) part is shown by solid (dashed) line. (c) Modulation of magnetic field strength $h = B_{\theta}/B$ for the tokamak (dashed line) and LHD (solid line).

with radial label, and local quantities like local shear and curvature are changed with the field line label, so that the change of these parameters is expected to affect the stability. Nevertheless, the above results show that these effects are weak, and the radial growth rate curve seems to be mainly determined by $k_{\perp}\rho_{thi}$ value, as can also be seen by comparing with Fig. 1. Then the core region is stabilized by the ion FLR effects and the edge is also stabilized by the small $k_{\perp}\rho_{thi}$.

Typical ITG eigenfunctions in LHD and our tokamak case are compared in Fig. 3. It can be seen that the mode width along a field line is not so different in LHD and the tokamak, and the modes are not confined in a helical ripple but in a toroidal period.

From above, the modes at $\theta_k \sim 0$ are not so different in LHD and the comparable tokamak. However, the slight difference can be found when ballooning angle θ_k is changed. The results are plotted in Fig. 4 for LHD (left) and

comparable tokamak (right). In this figure, we also show a case that ω_d is ignored which is denoted by triangles. The instabilities in this case are driven by the parallel compressibility, as already mentioned in Fig. 1. As is reasonable, the growth rates are same level for LHD and the tokamak when ω_d is nonexistent. In the tokamak case, the comparison with or without ω_d shows that ω_d is unfavorable in the outer side of torus with $\theta_k \sim 0$, while it becomes favorable in the inner side as θ_k increases. On the other hand, in the LHD case, ω_d is always unfavorable. This is because the locally unfavorable curvature extends to the inner side of torus in the LHD, which is reflecting the magnetic hill nature.

3. TEM cases

In Fig. 5 (left), we show the frequencies of TEM as a function of $k_{\perp}\rho_{thi}$ in LHD. A case for eliminating non-adiabatic ions is also plotted by open circles, and it can be

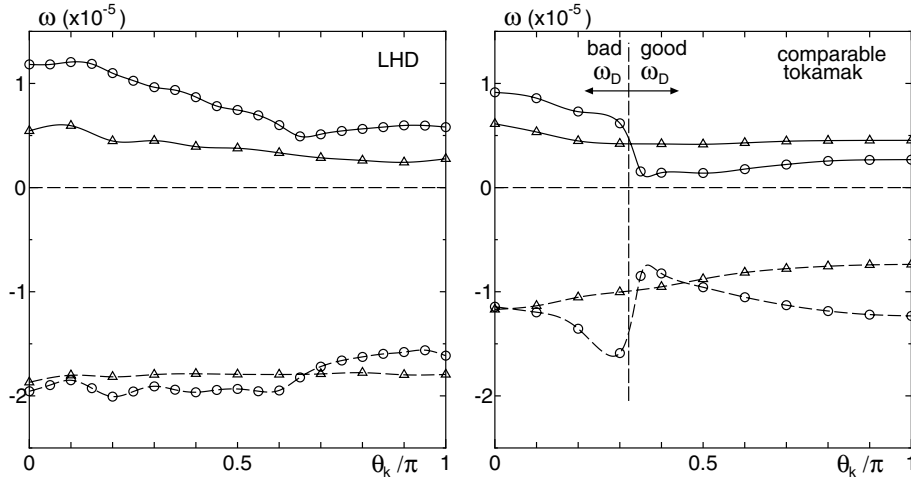


Fig. 4 θ_k dependence of ITG frequencies in LHD (left) and comparable tokamak (right), at $s = 0.7$. Real frequency and growth rate is shown by dashed and solid line with circles. Triangles also show cases that magnetic drift frequency ω_d is ignored.

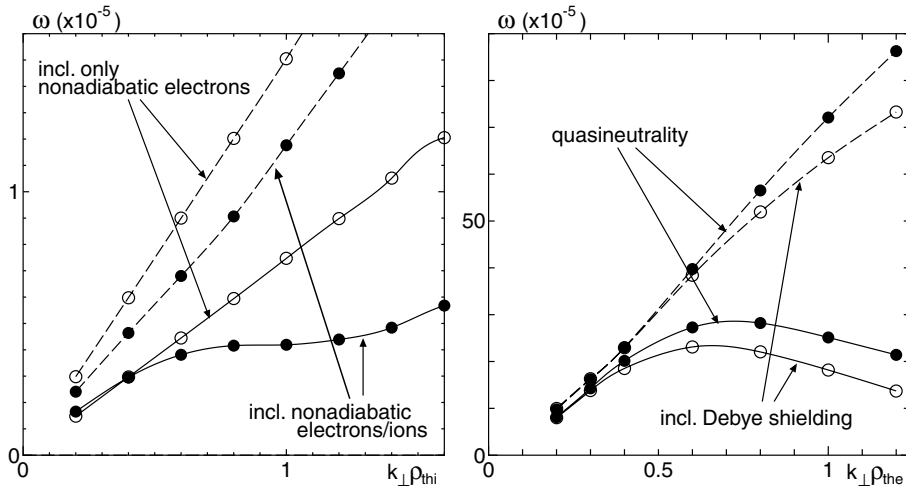


Fig. 5 $k_{\perp}\rho_{thi}$ dependence of TEM frequencies in LHD. Local parameters are $(s, \theta_k, M\alpha) = (0.7, 0, \pi)$. Closed circles show a case of non-adiabatic ions and electrons, and open circles show a case of eliminating non-adiabatic ions. (Right) $k_{\perp}\rho_{the}$ dependence of ETG frequencies in LHD. Local parameters are $(s, \theta_k, M\alpha) = (0.7, 0, \pi)$. Closed circles show a case for quasi-neutrality condition, and open circles show a case for including Debye shielding effect. Solid (dashed) line shows the growth rate (real frequency) for both figures.

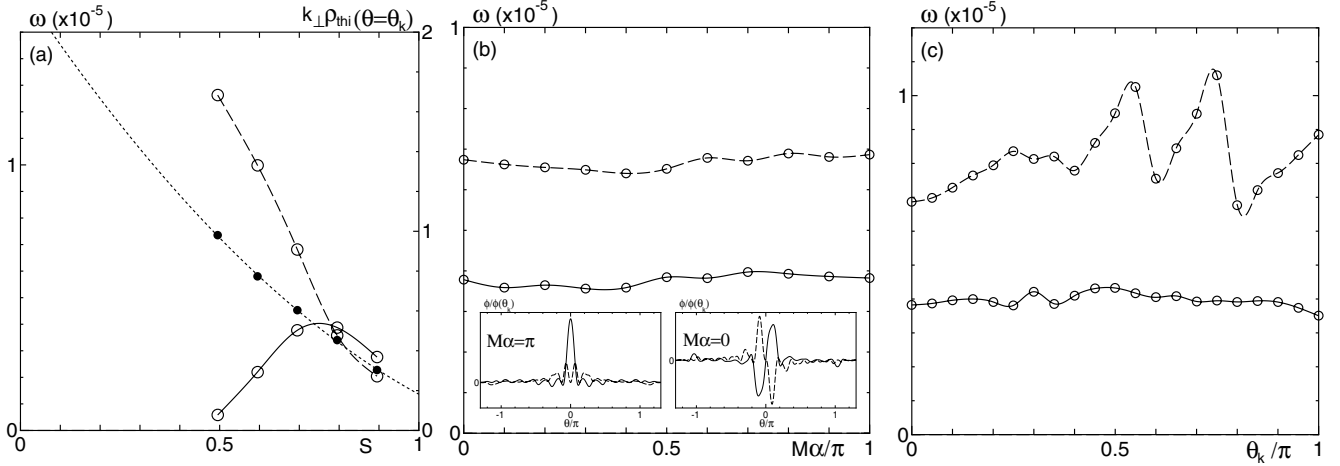


Fig. 6 (a) Radial dependence, (b) field line ($M\alpha$) dependence, (c) θ_k dependence of TEM frequencies with $n_k = 86$. Solid (dashed) line shows the growth rate (real frequency). Two of local parameters ($s, \theta_k, M\alpha$) = (0.7, 0, π) are fixed for each dependence plot. In (a), $k_{\perp}\rho_{thi}(\theta = \theta_k)$ value is also plotted by dotted line on right coordinate.

seen that the modes can be unstable in the absence of the non-adiabatic ions. This indicates that the electrons are essential for the instabilities, and this and positive ω_r indicate the modes are the TEM.

As can be seen, the increase of $k_{\perp}\rho_{thi}$ cannot stabilize the modes, unlike the case of ITG. This is reasonable because the ion FLR effect should not work for the electron-dominated dynamics. By comparing the cases with or without the non-adiabatic ions, the non-adiabatic ions are found to be stabilization, contrary to the role of the non-adiabatic electrons for the ITG. The reason is now under consideration.

In Fig. 6(a), the radial dependence of TEM frequencies is shown. Here the value of $k_{\perp}\rho_{thi}(\theta = \theta_k)$ is also shown on right-Y axis. From the Fig. 5 (left), the mode is not stabilized by the increase of $k_{\perp}\rho_{thi}$ unlike the ITG, so that the stabilization in the core cannot be explained by the high value of $k_{\perp}\rho_{thi}$. Thus in this case, the reduction of trapped electron fraction is responsible for this.

The θ_k and $M\alpha$ dependences of frequencies are shown in Figs. 6(b) and 6(c). For both cases, the frequencies have very weak dependence on these parameters. For the TEM cases, this is because the modes are very localized in a helical ripple, and the modes can find another ripple to localize when the θ_k or $M\alpha$ is changed. This can be seen in the eigenfunction structure as shown in Fig. 6(b). Here $M\alpha$ is changed as π and 0 which correspond to locally unfavorable and favorable curvature for $\theta \sim \theta_k = 0$. For the $M\alpha = 0$ case, the eigenfunction is odd, and it can localize in the neighborhood bad curvature region.

4. ETG cases

The ETG modes can also be destabilized by electron temperature gradient. The dynamics is almost the same as the ITG, because two types of instabilities can be treated merely by scale transformation, when ITG/ETG is considered to be driven only by ions/electrons.

Possible changes between the ITG and ETG come from:

(i) non-adiabatic electrons can contribute to the ITG as

discussed in Sec. 2, and (ii) spatial scale of ETG can become comparable to the Debye length so that the Laplacian term in the Poisson equation (Debye shielding term) is not negligible.

To investigate the latter, we show the ETG frequencies as a function of $k_{\perp}\rho_{the}$ in Fig. 5 (right), in cases with or without the Debye shielding term. Here we consider only electron species because it turned out that the bounce frequency of ions is too small compared to the dynamics; $\omega/\omega_{bi} \gg 1$ and a divergent problem often occurs numerically. However, it seems not so wrong to ignore the ion contributions because the ion FLR effect should already eliminate the ion's significance in this high wave number regime.

It can be seen that the Debye shielding gives an additional stabilization as $k_{\perp}\rho_{the}$ increases. On the other hand, it is negligible for $k_{\perp}\rho_{the} \leq 0.3$ and this indicates that the quasi-neutrality condition is well satisfied for the ITG or TEM regime. Here we fix the beta value in these calculations, however, the Debye shielding effects also strongly affect the stability at the low beta (or low density), as can be understood from the definition of the Debye length, $\lambda_D^2 = \epsilon_0 T_e / (e_e^2 n_e)$. The other properties of ETG are expected to be resemble to the ITG.

5. Conclusions

As a first step of linear stability analysis of electrostatic drift modes in LHD, the linear gyrokinetic-Poisson mode equation is solved in a numerically obtained equilibrium with a fixed temperature and density profile, and the results are compared to a circular tokamak with the comparable aspect ratio and the same magnetic shear (safety factor) profile.

The ITG modes are found to be unstable for $k_{\perp}\rho_{thi} \geq 1$. The radial dependence of the ITG frequencies is considered to be determined by $k_{\perp}\rho_{thi}$ so that the modes are stabilized in the plasma core with high $k_{\perp}\rho_{thi}$, and they are also stabilized at the edge with low $k_{\perp}\rho_{thi}$. The comparison with a tokamak with comparable aspect ratio shows that the ITG modes in LHD have similar properties to those in the tokamak. The

reason is that the local (toroidal or helical) curvature destabilization is dominated by the slab-like parallel compressibility because the negative q' shear tends to reduce the toroidal effects for the ballooning-like instabilities, and the slab-like mechanism is common effect in the torus as well as slab configurations. In addition, the large temperature gradient $\eta = 5$ also makes the instabilities very strong. Thus both the negative q' and large η assumed in this study are responsible for the similarity of ITG properties in LHD and the tokamak.

The TEM can also be destabilized for $k_{\perp}\rho_{thi} \gtrsim 1$. Unlike the ITG, the eigenfunction of the TEM is strongly localized in a helical ripple $2\pi/M$, and thus the modes should be strongly affected by the local magnetic structure. Nevertheless, the local parameter (θ_k, α) dependence is found to be weak. This is because the modes can find another helical ripple to localize when these parameters are changed. The TEMs with a fixed toroidal mode number are stable in the core because the trapped electron's fraction becomes small as in the tokamak. As a result, both the ITG and the TEM tend to be stable in the core, although the stabilizing mechanisms are different. It is noted that the TEMs are usually stabilized in the negative q' tokamaks, so that the TEM results here are considered to be inherent to the LHD.

Its importance in the LHD experiments should be studied in details.

The ETG can also be destabilized for $k_{\perp}\rho_{the} \gtrsim 1$. In addition to the electron FLR effects, the Debye shielding effects can also give stabilization for the ETG. Except for the differences of the temporal and spatial scales associated with the mass ratio, the ETG would be rather resemble to the ITG, at least for the linear electrostatic gyrokinetic analysis, as can be checked by normalizing the gyrokinetic-Poisson equations appropriately.

Acknowledgements

One of the authors (OY) thanks Dr. Yasuhiro Idomura for fruitful discussions.

References

- [1] A. Iiyoshi, A. Komori, A. Ejiri *et al.*, Nucl. Fusion **39**, 1245 (1999).
- [2] G. Rewoldt, W.M. Tang and M.S. Chance, Phys. Fluids **25**, 480 (1982).
- [3] M. Kotschenreuther, G. Rewoldt and W.M. Tang, Comput. Phys. Commun. **88**, 128 (1995).
- [4] S.P. Hirshman, Phys. Fluids **26**, 3553 (1983).